EPJ manuscript No.
(will be inserted by the editor)

First direct mass measurements of neutron-deficient xenon isotopes using the ISOLTRAP mass spectrometer

J. Dilling[1] [a], F. Herfurth[2], A. Kellerbauer[2], G. Audi[3], D. Beck[1], G. Bollen[4], S. Henry[3], H.-J. Kluge[1], D. Lunney[3], R.B. Moore[5], C. Scheidenberger[1], S. Schwarz[4], J. Szerypo[6], and the ISOLDE Collaboration[2]

[1] GSI Darmstadt, Postfach 110552, D-64220 Darmstadt, Germany

[2] CERN, CH-1211 Geneva 23, Switzerland

[3] CSNSM-IN2P3-CNRS, F-91405 Orsay-Campus

[4] NSCL/MSU, East Lansing, South Shaw Lane East Lansing, MI 48824-1321, USA

[5] Physics Department, McGill University, Montreal, H3A 2B1, Canada

[6] JYFL, University of Jyväskylä, Fin-40351 Jyväskylä, Finland

Received: date / Revised version: date

Abstract. The masses of the noble gas Xe isotopes with $123 \geq A \geq 114$ have been directly measured for the first time. The experiments were carried out at the ISOLTRAP triple trap spectrometer at the on-line mass separator ISOLDE/CERN. A mass resolving power of the Penning trap spectrometer of $m/\Delta m \approx 500000$ was chosen and an accuracy of $\delta m \approx 12\,keV$ for all investigated isotopes was achieved. Conflicts of several standard deviations with existing indirectly obtained mass data were found and are discussed. An atomic mass evaluation has been performed and the results of this adjustment are compared with results obtained for laser spectroscopy experiments. Drastic nuclear effects do not appear in the region of investigation. Particularly, nuclear shape-coexistence could not be confirmed.

PACS. PACS-key describing text of that key – PACS-key describing text of that key

1 The ISOLTRAP mass spectrometer

1.1 Experimental set-up

The ISOLTRAP Penning trap spectrometer [2,3] is installed at the on-line facility ISOLDE/CERN in Geneva.

[a] *Corresponding author* (present address: TRIUMF, 4004 Wesbrook Mall, Vancouver, B.C., V6T 2A3 Canada, E-mail: JDilling@triumf.ca)

Exotic nuclei are produced via proton bombardment of a thick target. The products created by spallation, fragmentation or fission reactions are ionized, extracted and mass separated. The quasi-continuous beam of typically $30-60\,keV$ is subsequently transported to the ISOLTAP experiment.

The ISOLTRAP experiment consists of three electromagnetic traps which serve different purposes. The first trap is used to stop, cool and transform the continuous beam into a low-energetic ($E_{kin} \approx 2.5\,keV$) ion bunch. The second trap acts as an isobar separator and the third is a high-accuracy mass spectrometer. Figure 1 shows the set-up of the triple-trap spectrometer.

The first trap, a linear gas-filled radiofrequency quadrupole (RFQ) trap [4] of about 1 meter length catches the ISOLDE beam. The trap is sitting on a $60\,kV$ high voltage platform and therefore the beam is electrostatically retarded. By interacting with the buffer gas the ions are cooled to thermal temperature. Potential walls at the end-section allow accumulation of the ions. By switching these electric fields the ions can be extracted as a low energetic bunched beam.

The cooler trap is a large ($\oslash_{in} \approx 32\,mm$) cylindrical Penning trap, sitting in the homogeneous field of a 4.7 T superconducting magnet. This trap is used to further clean the ion sample by applying mass-selective buffer gas cooling [2,5]. In a Penning trap, interaction with the buffer gas leads to larger magnetron radii resulting finally in a loss by hitting the ring electrode. If however, a radiofrequency azimuthal quadrupole field of the proper strength

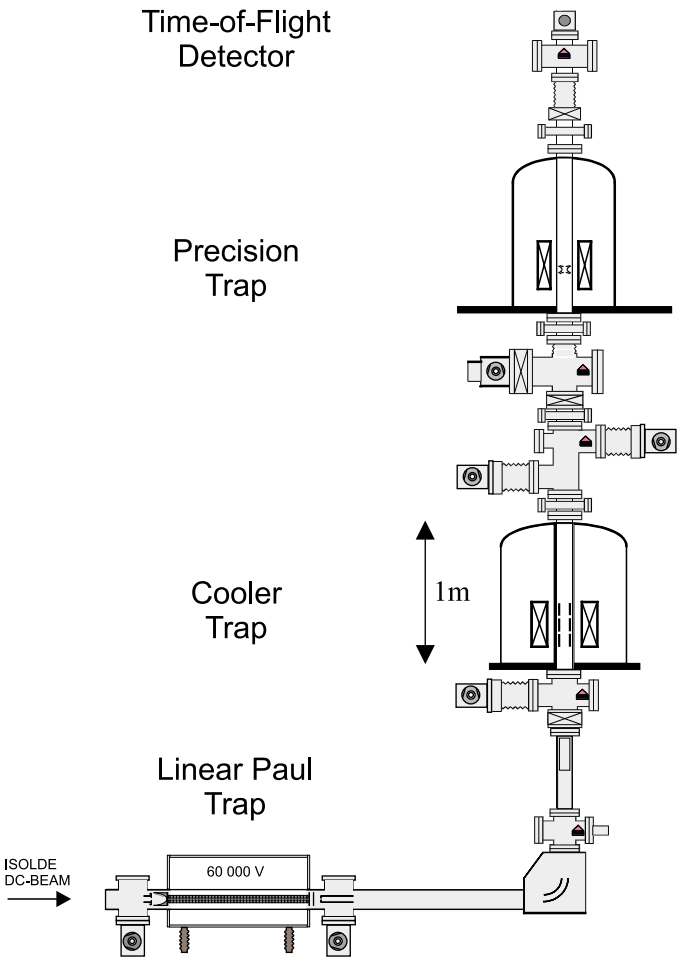

Fig. 1. Experimental set-up of ISOLTRAP. The linear Paul-trap is used for cooling and bunching of the ISOLDE beam. The cooler-trap acts as an isobar separator. The high-accuracy mass measurement is performed in the precision trap by employing a time-of-flight technique.

and frequency is applied, the ions of choice are cooled to the center of the trap. They are then gently extracted and delivered to the third trap.

This precision trap is a hyperbolical Penning trap in a B =6 T field of a second superconducting magnet. An azimuthal radiofrequency (rf) field is applied. The absorption of the mass depending frequency ω_{rf} leads to a gain in azimuthal energy. After the excitation process the ions are

ejected from the trap towards a particle detector. During the drift through the inhomogeneous part of the magnetic field the azimuthal energy is converted to an axial energy due to the orbital magnetic moment. Therefore the ions excited by the applied rf-field reach the detector faster than the others. Hence the time of flight from the trap to the detector can be used to measure the cyclotron resonance. The equation

$$\nu_c = q/m \cdot B/2\pi, \tag{1}$$

relates the resonance cyclotron frequency ν_c to q/m, the charge to mass ratio of the ions. The magnetic field B is calibrated by using a reference isotope with well known mass. Since only singly charged ions are delivered to the precision trap, the knowledge of the magnetic field enables the determination of the mass of the ions. Figure 2 shows a time-of-flight spectrum as a function of applied radiofrequency. The solid line is the theoretical expected shape of the resonance [6] fitted to the data points.

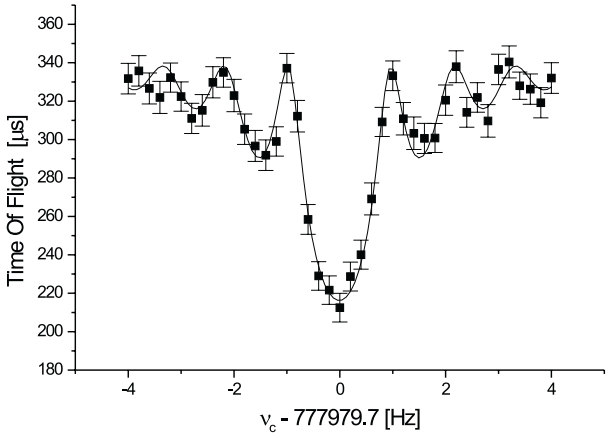

Fig. 2. Cyclotron resonance curve for ^{117}Xe. Depicted is the time of flight of the ions from the trap to a detector as a function of applied radiofrequency. The solid line is a fit of the theoretically expected shape [6] to the experimental points.

1.2 Beam preparation in the linear Paul trap

The measurements of noble-gas isotopes reported in this paper were only possible after the recent installation of the linear Paul trap [4]. This RFQ trap, about 1 meter long, is filled with He buffer gas at a pressure of $p \approx 2 \cdot 10^{-2}\, mbar$ and placed on a high-voltage (60 kV) platform. This device replaces the previous system for the preparation of ions by implantation of the ISOLDE beam in a hot foil and reionization. The very successful experimental program of ISOLTRAP, determining more than 200 isotopes to date (see for example [7–9]) could now be extended and non-surface ionizable species become accessible.

One of the critical points in this device is the loss of singly charged ions due to charge exchange processes. In the beginning of the experiments the xenon ions did not survive the transfer to the first Penning trap. Therefore the vacuum conditions had to be improved and the buffer gas further purified in order to obtain a sufficient survival time of the singly charged ions in the buncher. Figure 3 shows the number of extracted ions as a function of storage time in the RFQ trap. The decay constant is $\tau = 210\, ms$, which is an improvement by a factor of five over that previously obtained. This was reached by heating the RFQ system for several hours and including a cold trap into the feeding line of the buffer gas. Both measures led to a decrease of contaminants in the residual gas. Interac-

tions with these impurities are the dominant effect for the neutralization processes of the xenon isotopes and consequent loss. The charge exchange cross section is maximized for a resonant process, with $IP_A - IP_B = \delta E = 0$, and IP_A and IP_B are the ionization potential of the ion under investigation and neutral atom or molecule causing the charge exchange. The ionization potential of xenon is $IP_{Xe} = 12.1\,eV$. Therefore possible candidates for such a process would be: O_2 (12.1 eV) or CH_4 (12.5 eV). Both are present in the residual gas in vacuum systems. For further improvements of the survival time in the RFQ system, a higher level of purification of the vacuum system has to be reached.

Thermal equilibrium of xenon ions with the buffer gas is reached after $T_{cool} \approx 10\,ms$ [4]. In this beam time cooling was applied for $10-20\,ms$. The remaining 95 % of the ions were then ejected as a bunched beam with an improved emittance [4] at a transfer energy of $E_{trans} = 2.5\,keV$.

1.3 Obtaining an isobaric pure sample

The ISOLDE facility offers two magnetic separators. For the experiments reported here the general purpose separator (GPS) [11] was used with a mass resolving power of about $R = m/\Delta m_{FWHM} \approx 1200$. With this resolution isobaric contaminations can not be excluded and the ion cloud has to be cleaned from isobars in the cooler trap (fig. 1). In the experiments presented here isobars of Cs, In, Sn, I and even molecules like InO had to be considered. A cleaning procedure to remove impurities was therefore performed. A dipole field at the mass insensitive magnetron frequency ω_- is applied at the cooler trap with a duration of $T_{RF} = 20\,ms$. The magnetron motion of all stored ions is excited leading to an increase of the radius of the motion. Then the centering only of the investigated isotopes with a duration of $T = 100\,ms$ was started at their cyclotron frequency ω_c. In this way the resulting resolving power of $m/\delta m_{FWHM} \approx 70000$ allows a clean sample to be delivered to the precision trap.

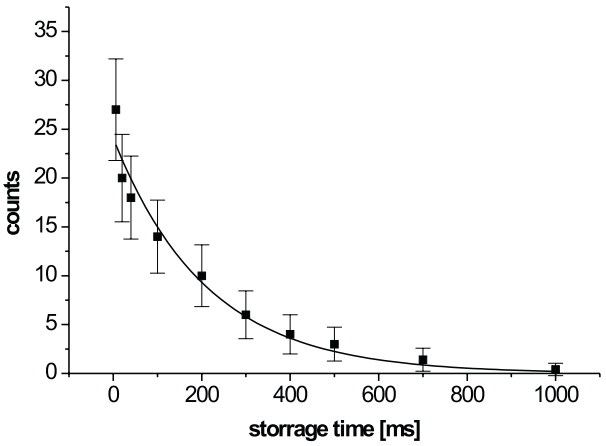

Fig. 3. Losses of stable $^{130}Xe^+$ ions in the buncher as a function of storage time. The decay constant is $\tau = 240 \pm 24\,ms$. The loss is mainly due to charge exchange.

2 Measurements

The data in this work have been obtained during one online run. A La_2O_3 target was bombarded by a 1 GeV proton beam with a current of 1 μA. It was coupled via a cold transfer-line to a plasma ion source. In this way the volatile isobars were drastically reduced.

2.1 Efficiency

The overall efficiency of the experiment was determined by measuring the intensity of the ion beam in the focal plane of the GPS separator of ISOLDE and in front of the ISOLTRAP experiment, directly downstream from the buncher, with standard Faraday cups. This currents were compared with the number of detected ions at the time-of-flight particle detector of ISOLTRAP. For the transfer efficiency from the GPS to the experiment a value of $\epsilon = 93^{+7}_{-15}\%$ was found. For the entire transfer from the separator to the TOF-detector behind the precision trap the overall efficiency was $\epsilon = (2.0 \pm 0.3) \cdot 10^{-4}$, corresponding to an improvement of a factor of 1000 to the previously used set-up. Detailed investigations show that the transmission could be significantly improved at three of the stages in the transfer. Whereas the efficiency of $\epsilon \approx 25\%$ is acceptable for the buncher, the transfer efficiency from the buncher to the cooler trap is only $\epsilon = 1\%$ and the transfer between the Penning traps is $\epsilon = 10\%$. Here, investigations of necessary changes, mainly in the ion optics, are currently under way. An improvement by at least a factor of 50 seems to be feasible.

2.2 Production yield

The production yield of the xenon isotopes was measured in the focal plane of the ISOLDE separator. For those isotopes, where the produced ion beam was too weak to be measured directly with a standard Faraday cup, the production yield was determined via the TOF-detector of the precision Penning trap, assuming constant transport and detection efficiency. Figure 4 shows the production yields of the xenon isotopes. This can be compared to the measurements in [12], where the yields are given for a 600 MeV proton beam at 1 μA and which are slightly higher. This is probably due to the low ionization efficiency of the plasma ion source, only about 3% [13] during the actual beam time. Usually such ion sources have an ionization efficiency of $30 - 40\%$ [14]. The yields in [12] were only determined for xenon masses with $A \geq 116$, whereas the new data go further to lower mass number $A = 114$. The genereal trend is changing here and some saturation seem to set in. This is most likely artificial, since a yield drop of approximately one order of magnitude per missing neutron could be expected. A possible explanation is the change in ionization

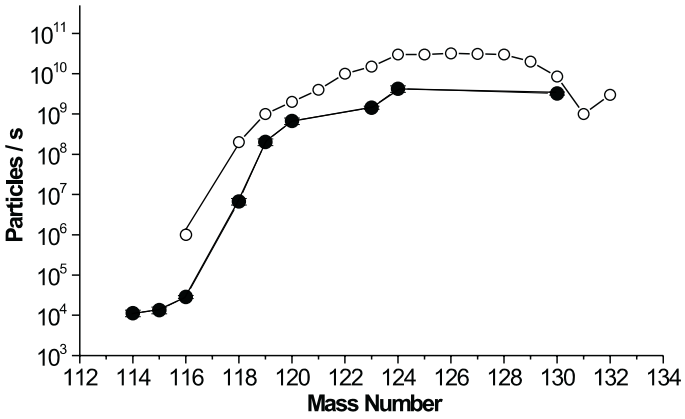

Fig. 4. Yields for the production of Xe isotopes in the focal plane of the GPS separator of ISOLDE created by bombarding a La_2O_3 target with a $1GeV/1\mu A$ proton beam. Constant transport efficiency of the apparatus is assumed. Open circles taken from [12], solid points from the presented data. For further explanation see text. The connecting lines are only to guide the eye.

efficiency of the ion source since the data were not taken in chronological order.

2.3 Mass Measurement

2.3.1 Measurement Procedure

Mass measurements of neutron deficient xenon isotopes with $114 \leq A \leq 124$ and $A = 130$ were carried out in the present experiment. The measurement procedure includes the preparation in the RFQ trap (10 ms), the purification in the cooler trap (120 ms) and the measurement in the precision trap. In this last step the ions are excited for $T_{RF} = 900\,ms$ by an rf-field at a given frequency. The complete cycle is then performed 41 times (supercycle) at equidistant rf-frequencies in the precision trap to determine the resonance (fig. 2). The resonance width $\Delta\nu_{FWHM}$ is approximately equal to the inverse of the excitation period T_{RF}. For example, for $A = 120$ the cyclotron frequency is $\nu_c = 760\,kHz$ in a magnetic field of $B = 6\,T$. Using an excitation time of $T_{RF} = 900\,ms$ a width of $\Delta\nu_{FWHM} \approx 1.1\,Hz$ can be reached. This corresponds to an resolving power $R = m/\delta m \approx 10^6$, allowing mass measurements with a accuracy of $\delta m/m \approx 1 \times 10^{-7}$.

2.3.2 Frequency ratios

The cyclotron frequency is obtained by fitting the theoretical shape of the resonance [6] to the measured time-of-flight spectrum (fig. 2). The center frequency, the FWHM, and the statistical uncertainty are deduced. For the conversion into an atomic mass the magnetic field has to be known. This is accomplished by loading stable reference ions of very well known mass into the spectrometer and measuring the cyclotron frequency. The ratio of the two measured frequencies $R = \nu_{ref}/\nu$ can be given as the primary experimental result. Table 1 shows the measured isotopes together with the frequency ratio with respect to ^{133}Cs ions. In the first brackets the statistical and in the second brackets the total error are shown. The statistical error here depends on the number of detected ions, given by the maximum number of ions detected per cycle (column 3) and the number of supercycles (column 4) per measurement. For example, for ^{119}Xe the number of ions detected in one cycle was 5. For 38 supercycles this corresponds to a total of $5 \cdot 41 \cdot 38 = 7790$ ions. The average number of detected ions per isotope was $\hat{N} \approx 5000$ in the experiments presented here. Including the resolving power of the spectrometer, the expected statistical uncertainty can now be approximated

$$\delta\nu/\nu = (1/R) \cdot (1/\sqrt{\hat{N}}) = (1/500000) \cdot (1/70.7) = 3 \cdot 10^{-8}. \quad (2)$$

The total error is given as the quadratic sum of the statistical and systematic error. The sources of systematic errors considered are the following:

- Frequency shifts due to magnetic field imperfections. These systematic errors are proportional to the mass difference between the reference ions and the ions under investigation. This difference is maximum at δA =19 amu (for ^{114}Xe). For ISOLTRAP mass measurements this shift was investigated in [17] to be $2 \cdot 10^{-9}$/amu,

Table 1. Mass data of xenon isotopes measured by ISOLTRAP. The frequency ratio of the singly-charged xenon isotope to the reference ($^{133}Cs^{+}$) together with statistical and total error is listed in column two. In the next columns the maximum number of detected ions per cycle (#N), the number of supercycles (#S) for the time of flight measurements and in the next column the half-life is shown. The mass excess (column 6) derived from the Penning Trap (ME(PT)) frequency ratio and the literature (AME [10]) value together with the corresponding absolute error are given in column 7. Values marked (#) are estimates from systematic trends [10]. In the last column the difference (dev) between those two values is shown (dev = ME(PT) - ME(AME)).

Nuclide	Freq.Ratio $\nu_{Ref.}/\nu$	Nr.ions	Nr.scyls.	$T_{1/2}$	ME(PT) [keV]	ME(AME) [keV]	dev [keV]
^{114}Xe	0.8572101482 (34) (93)	1	77	10 s	-67086 (12)	-66933 # (207#)	-153
^{115}Xe	0.8647216374 (32) (95)	1	73	18 s	-68657 (12)	-68426 # (239#)	-231
^{116}Xe	0.8722103533 (42) (109)	1	71	59 s	-73047 (13)	-72901 # (246#)	-146
^{117}Xe	0.8797253356 (19) (91)	9	19	61 s	-74185 (11)	-73994 (180)	-191
^{118}Xe	0.8872180141 (24) (93)	8	23	3.8 m	-78084 (12)	-77710 (1000)	-374
^{119}Xe	0.8947364709 (33) (91)	5	38	5.8 m	-78793 (11)	-78660 (123)	-133
^{120}Xe	0.9022333721 (40) (102)	1	52	40 m	-82170 (13)	-81832 (44)	-338
^{121}Xe	0.9097551270 (33) (100)	4	28	40.1 m	-82469 (12)	-82539 (24)	70
^{122}Xe	0.9172560020 (29) (99)	10	19	20.1 h	-85355 (12)	-85185 (87)	-169
^{123}Xe	0.9247811247 (40) (100)	4	25	2.08 h	-85237 (12)	-85260 (15)	23
^{124}Xe	0.9322857418 (22) (97)	9	25	stable	-87658 (12)	-87658 (2)	0
^{130}Xe	0.9774128763 (27) (101)	8	11	stable	-89878 (13)	-89881 (1)	3

corresponding to a maximum shift of $4 \cdot 10^{-8}$.

– Contaminating ions of different mass in the measurement trap. Investigations at ISOLTRAP [18] showed that these effects can cause an error of up to $\delta m/m \approx 10^{-7}$ if many ions are stored simultaneously in the trap ($\geq$ 25 ions detected by the TOF detector) and if the mass difference between contaminant and investigated ions is smaller than the resonance width $\Delta\nu_{FWHM}$. This was prevented by always having very few ions in the precision trap. Table 1 (column 3) shows the maximum number of detected ions per cycle.

– Temporal variations of the magnetic field which are not canceled out by the reference measurements. These can arise, for example from changes of the air pressure or the ambient temperature. Typically a day-night shift of $\delta B/B \approx 10^{-7}$ was found [17]. The measured average variation in the on-line experiments was $\delta B/B = 3 \cdot 10^{-8}$ for 11 reference measurements during the 28 hours duration of the experiment.

The total contribution of these systematic errors is below $1 \cdot 10^{-7}$. Nevertheless a conservative estimate of $1 \cdot 10^{-7}$ for systematic errors is added quadratically to the statistical error, which is on the order of $3 \cdot 10^{-8}$. Since a cycle time of $T_{cycle} \approx 1.3\,s$ was used, corresponding to a supercycle time of $T_{scycle} \approx 50\,s$, the average time for determining the frequency ratio of one isotope was $\hat{T} \approx 30\,min$.

2.3.3 Mass values

The conversion of the frequency ratio into an atomic mass is done by multiplying with the mass of the reference atom m_{ref}, and adding the rest mass of the electron m_e,

$$m = (\nu_{ref}/\nu) \cdot m_{ref} + m_e, \tag{3}$$

where is $m_{ref} = m_{ref}(atom) - m_e$, because here the atom is used as reference but ions are measured. For the presented data ^{133}Cs was used for this purpose, for three reasons. Firstly, the mass was recently determined [19] with a relative uncertainty of $\delta m/m = 2 \cdot 10^{-10}$. Secondly the mass difference between the reference ions and the xenon ions is small. And thirdly, because of to the possibility of producing them from the internal test ion-source, independently of the ISOLDE facility.

By using the frequency ratio and the known mass of the reference ions the mass can be given as the physics result. The mass excess derived from that relation is given in table 1 (column 6) together with the final error. In the next column in table 1 the mass excess is given from literature values [10] or estimates (#) from systematic trends from therein.

The masses of the three isotopes ^{114}Xe, ^{115}Xe and ^{116}Xe were determined for the first time. For all measured unstable xenon isotopes the accuracy was drastically improved. The reliability and accuracy of the ISOLTRAP measurement can be tested in the cases of the stable isotopes ^{124}Xe and ^{130}Xe, which are known with an accuracy of about $1 \cdot 10^{-8}$. The deviation of the ISOLTRAP data from those values is $\delta m(^{124}Xe) = 1(12.5)\,keV$ and $\delta m(^{130}Xe) = 3(13)\,keV$, hence excellent agreement is observed.

3 Atomic mass evaluation and results

Within this work an atomic mass evaluation (AME) has been performed. A detailed description of such an evaluation can be found in [10]. The concept followed in this compilation is to use all available experimental mass data within a least-squares procedure of linear equations. Table 2 gives the result of the atomic mass evaluation. Listed are all nuclides whose mass values have changed by more than $10\,keV$ when including the new ISOLTRAP data. From the 12 directly measured xenon isotopes a total number of 18 isotopes were influenced notably. For the xenon isotopes some drastic shifts occurred in the mass excess values, going up to 7.7 standard deviations compared to the previous values of the AME. Figure 5 shows the difference of the atomic evaluation with and without the ISOLTRAP data. One clearly notices the dramatic change in accuracy reached now with the new ISOLTRAP values, which is for all measured xenon isotopes on the or-

Table 2. Results of the atomic mass evaluation. The nuclides are listed in column 1. The mass excess values from two least-squares adjustment are given in columns 2 (AME 95) and 3 (AME new, including the Penning trap data) with the total error in brackets. The deviation between both is listed in column 4. Values marked with # are estimations from systematic trends [10].

Nuclide	AME 95 [keV]	AME new [keV]	dev [keV]
^{114} Xe	-66933.0 # (207.0#)	-67086.2 (11.0)	-153.2
^{115} Xe	-68426.0 # (239.0#)	-68657.0 (12.0)	-231.0
^{116} Te	-85305.7 (92.0)	-85288.3 (95.0)	14.4
^{116} I	-77560.5 (142.6)	-77543.2 (144.6)	17.4
^{116} Xe	-72901.0 # (246.0#)	-73047.0 (13.0)	-146.0
^{117} I	-80436.5 (71.1)	-80447.1 (72.4)	-10.5
^{117} Xe	-73993.6 (179.9)	-74184.7 (11.0)	-191.1
^{117} Ba	-56952.0 # (648.0#)	-57098.0 # (600.0#)	-146.0
^{118} Xe	-77709.7 (1000.1)	-78084.7 (11.0)	-375.0
^{119} I	-83666.0 (63.4)	-83671.5 (64.8)	-5.5
^{119} Xe	-78659.9 (123.4)	-78793.0 (11.0)	-133.1
^{119} Ba	-64220.8 (1019.9)	-64595.8 (200.3)	-375.0
^{120} Xe	-81831.5 (44.0)	-82169.5 (13.0)	-338.0
^{121} Xe	-82539.3 (24.4)	-82468.9 (12.0)	70.4
^{121} Cs	-77139.3 (13.9)	-77068.9 (23.4)	70.4
^{121} Ba	-70342.5 (303.2)	-70680.6 (300.3)	-338.0
^{122} Xe	-85185.2 (87.3)	-85354.5 (12.0)	-169.3
^{123} Xe	-85259.9 (15.4)	-85245.5 (9.0)	14.4

der of $\delta m \approx 12\,keV$. For the isotopes $A = 114, 115$ and 116 only estimated values existed, which could now be replaced by high-accuracy experimental data. It is however notable that those estimated AME 95 values agree well within their (large) error bars with the now measured values. This is in contrast to previously experimentally determined masses used for AME 95, closer to the valley of stability, namely for ^{120,121,123}Xe. One notices also that most of the previous masses were too small. This can be explained by systematic errors made by determining the masses at on-line facilities, where the background could probably not be sufficiently suppressed. A detailed com-

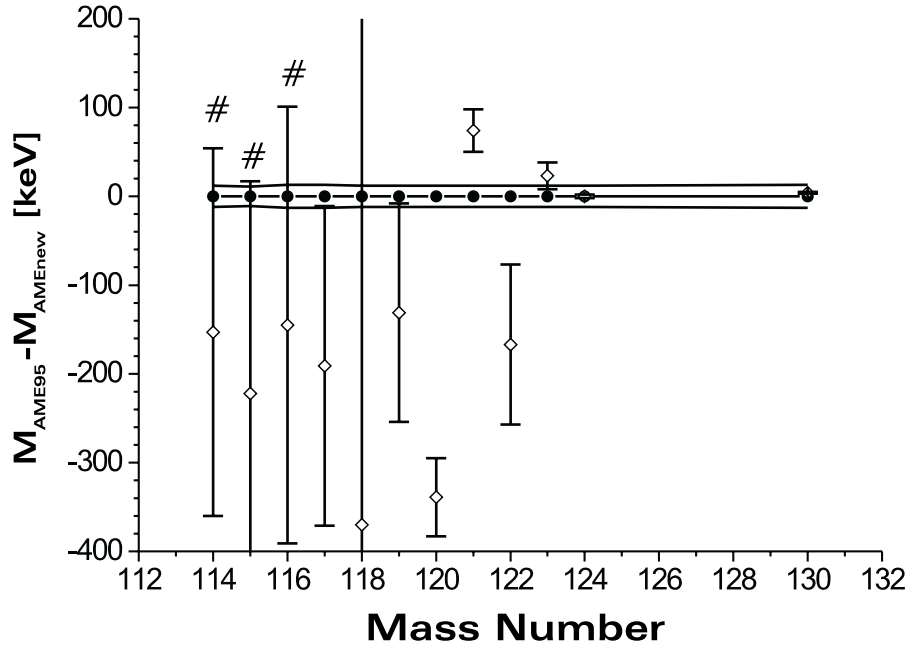

Fig. 5. Difference between xenon mass values from the Atomic Mass Evaluation 1995 (AME 95) [10] (data points with error bars) and an evaluation including the ISOLTRAP data (zero line with error band). For isotopes marked with # masses are estimated from the extrapolation of systematic trends [10].

parison between old and new input data is discussed in the appendix, where the conflicts are also discussed.

4 Discussion of the results of the new atomic mass evaluation

4.1 Two-neutron separation energies

The S_{2n} is defined as the difference in binding energy ($E^B(Z,N)$) for two isotopes differing in neutron number N by 2

$$S_{2n} = E^B(Z,N) - E^B(Z,N-2). \quad (4)$$

The two-neutron separation energy allows one to recognize changes in the nuclear structure without the complication of the huge odd-even effects such as pairing. Figure 6 shows the S_{2n} as a function of mass number A for the measured xenon chain and neighboring element where changes occurred due to ISOLTRAP data. This is the case for 23 S_{2n}-values, where at least one datum of the S_{2n} input was changed. The new values are plotted as solid points, the previous data taken from the AME 95 [10] as open circles. Generally, a very smooth behaviour of the two-neutron separation energies (especially for the nuclides with even proton number) is found in this region of the chart of nuclides, indicating the absence of any drastic nuclear structure effects in those neutron mid-shell nuclides. However at the neighboring chains of xenon some local irregularities appear, as in the case of ^{116}Cs at $N = 61$. For this isotope the binding energy is experimentally known with an uncertainty of $\delta m = 351\,keV$. The corresponding value

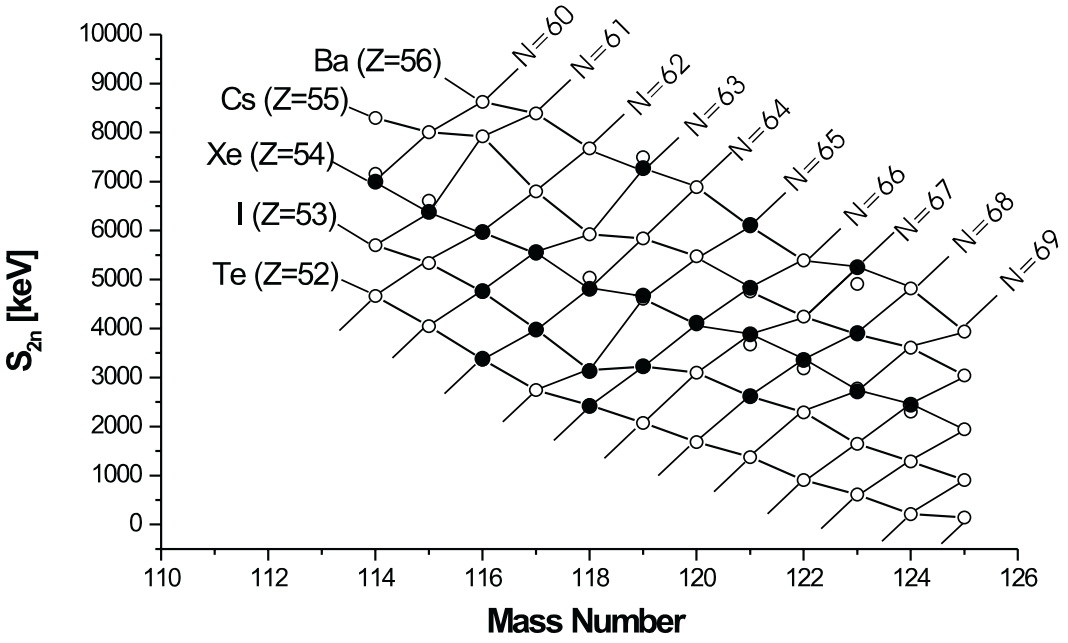

Fig. 6. Two-neutron separation energy S_{2n} as a function of mass number A. Filled circles show the new values, open circles old data calculated from AME [10]. No error-bars are shown.

of ^{114}Cs is an systematic estimate with $\delta m = 305\,keV$. That might be also the reason for the deviation at ^{118}Cs at N = 63, for which the ^{116}Cs-datum is also used. As a consequence, the mass of these Cs isotopes should be experimentally checked with good precision.

Another case for such a clear deviation from the general trend is found for iodine isotopes at $A = 118$. The experimental uncertainty of the two isotopes is $\delta m = 144\,keV$ and $\delta m = 72\,keV$, respectively. Again, better precision would be desired, to discriminate between an error in the input data or a nuclear structure effect.

4.2 Deformation effects within the xenon iobaric chain

Figure 7 (bottom) shows the two-neutron separation energies for xenon-isotopes with $114 \leq A \leq 141$. The S_{2n} is reduced by a linear function, in order to show nuclear shape effects more clearly. Besides the strong discontinuity observed at the shell closure at $N = 82$, a smoothly varying two-neutron separation energy is observed in the region $58 \leq N \leq 82$. Information on the quadrupole deformation can be obtained, for example, from isotope shift measurements known from collinear laser spectroscopy [22]. Figure 7 (top) shows the difference in the mean charge radius $\delta < r^2 >$ as a function of neutron number N (bottom scale) or mass number A (top scale). Also shown are equideformaton lines of $< \beta^2 >^{1/2}$-values at 0.1, 0.2 and 0.3 as calculated by use of a droplet model [21]. Comparing the reduced S_{2n} values with $\delta < r^2 >$, both graphs show a similar smooth trend from the very neutron-deficient isotopes towards the shell closure at $N = 82$ where a drastic change appears. In both cases a weak odd-even staggering is visible. The gradually increasing deformation for neu-

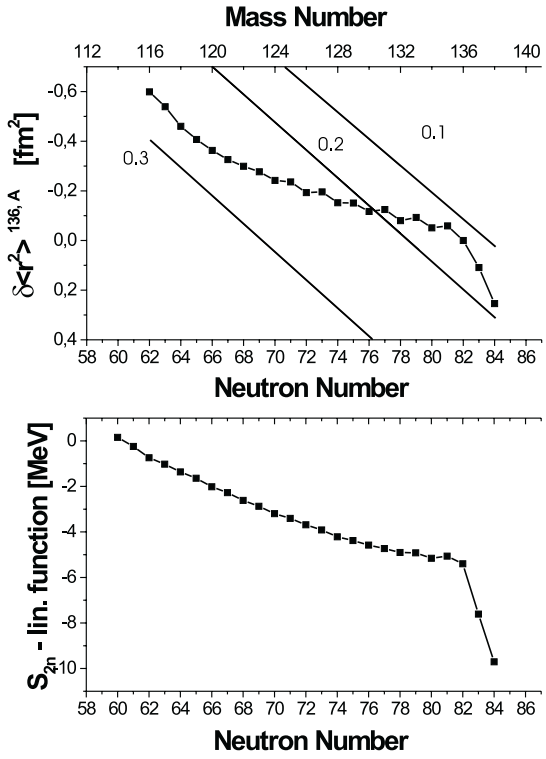

Fig. 7. Top: Mean charge radius difference of xenon isotopes with respect to ^{136}Xe (taken from [22]). Shown are also equideformation lines of $< \beta^2 >^{1/2}$-values at 0.1, 0.2 and 0.3 as calculated from a droplet model [21]. Lower: Reduced two-neutron separation energies for xenon isotopes derived from the measured mass data and AME.

tron numbers below $N = 82$ as obtained from the isotope shift data is obviously reflected in the bump of the S_{2n} values. No signature for a sudden transition appears, neither in the isotopes shift nor in the mass data. This is consistent with the description of a 'soft'-core by T.R. Werner and J. Dudek [23]. However, no fingerprints of shape-coexistence in the ground state could be observed. Shape-coexistence generated by a particle-hole intruder configuration is one of the suggested models for the enhanced E0 and E2 transition rates in the midshell Xe isotopes, particularly at $N = 64, 66$ and 68, found by P.F. Mantica and W.B. Walters [24]. Indications for such an effect would for example be deviations from the smooth trend, which are not found. Shape coexistence is often associated with isomerism [25]. Due to the high resolving power of the ISOLTRAP spectrometer isomeric states with energies higher than $120\,keV$ can be excluded. From the results presented here, nuclear shape coexistence can not be confirmed.

5 Conclusion and outlook

The xenon isotopes with $123 \geq A \geq 114$ have been directly measured for the first time using the ISOLTRAP triple trap spectrometer. The experimental precision could be increased drastically and is now $\delta m \approx 12\,keV$ for all nuclei investigated. For the isotopes ^{114,115,116}Xe values estimated from systematic trends, were previously used in the tables of the AME. This can now be replaced by high-accuracy experimental data. An atomic mass evaluation was performed and differences to the existing data were found, going up to several standard deviations. These conflicts were discussed in detail and could be solved. The new direct and indirect mass results are used to describe the mass landscape in the S_{2n}-picture. The measured xenon isotopes follow smoothly the general trend. Other chains show local deviations due to large experimental uncertainties. This could basically be overcome with the present ISOLTRAP set-up. Isotopes such as ^{116}Cs or ^{114}Cs with half lives $T_{1/2} = 700\,ms$ and $T_{1/2} = 570\,ms$ are now within reach of the experiment. A comparison of the reduced S_{2n}-values with the mean charge radius, shows the same trends

in nuclear structure. Shape-coexistence could not be confirmed based on the available ground state data. This is in accordance with recent theoretical investigations employing shell model calculations [26]. More detailed studies are needed.

The new RFQ linear cooler and buncher allowed for the first time, measurements on a chain of noble gases. In the near future, improvements on the vacuum system and the gas feeding should help to reduce losses in the RFQ due to charge exchange processes. Furthermore, the transfer efficiency will be improved by optimization of ion optics ans is expected to increase the total efficiency to $\epsilon \approx 1\%$. This will allow high-accuracy mass measurements even further from the center of the valley of stability, in a region where the production yield of exotic nuclei is very low.

APPENDIX

Discussion of the new input data set

In this section a detailed comparison between existing measurements and the new ISOLTRAP data is performed. All publications used or documented in previous atomic mass evaluations [10] were taken into account. For the evaluation the available data are carefully checked and categorized with regard to quality and /or documentation. In the evaluation the values are weighted in the linear equations accordingly.

^{123}Xe: For ^{123}Xe six previous mass measurements were used for the adjustment of the AME95 [10]. All were β-endpoint determinations. The most accurate one by R.B. Moore [28] (fig. 8 value #2) had the most influence in the AME 95 but disagrees by $1.5\,\sigma$ from the ISOLTRAP datum (fig. 8 value #7). R.B. Moore (as a co-author of this work) admits that the original error estimation of the β-endpoint measurement was eventually too small. For a second measurement there is also a $1.4\,\sigma$ deviation (fig. 8 #4). This datum is derived by K. Sofia et.al [30] by a linear fit to a Fermi-Kurie plot. The beta-spectrum is taken in coincidence with the $596.5\,keV\,\gamma$-line. The assigned error seems too small, since it looks possible on the viewgraph to fit linear functions to the data points, leading to endpoints outside the error interval. The other values for this isotope agree well with the ISOLTRAP datum within their error bars. For the new atomic mass evaluation the value given in [28] and [30] are excluded from the adjustment and marked with "Well-documented data which disagree with other well-documented values".

^{122}Xe: Five endpoint measurements were performed prior to the ISOLTRAP mass measurement of which two concern the very same experiment but different corrections concerning the isomeric state of the mother nucleus. One of those corrections [31] disagrees with our datum. The documentation of this experiment, a PhD thesis of the University of California, Berkeley, by R.F. Parry was not available, therefore a judgment of the quality was not possible. A discrepancy is also found with the experiment re-

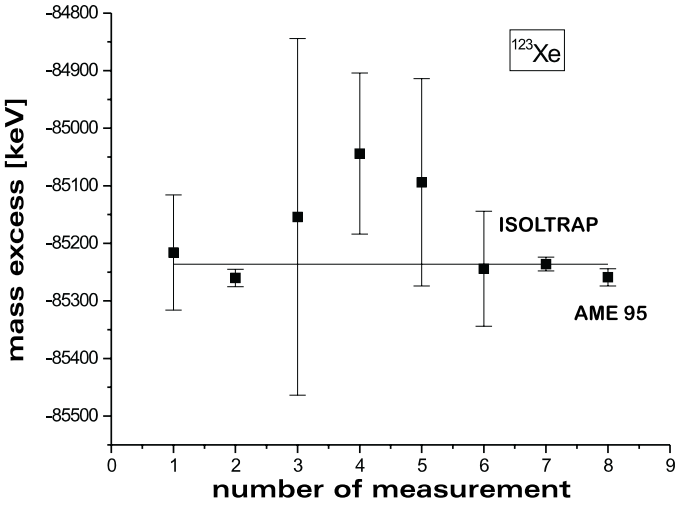

Fig. 8. Comparison of the ISOLTRAP value for ^{123}Xe with previously measured data of the mass excess and AME 95. The line indicates the value reported in this work. Measurement #1 [27], #2 [28], #3 [29], #4 [30], #5 [31], #6 [32].

ported by G.D. Alkhazov et al. [32]. Here the technique of β-decay energies determination via γ-ray endpoints was used, where a cascade of γ-rays is summed up in a total absorption detector. For this determination it is necessary to fully understand the beta-decay strength function $S_\beta(E)$ which is not the case for this isotope. Therefore this value is disregarded for the evaluation. The other experiments agree well within the given error.

^{121}Xe: Four of the six previously performed mass measurements of this nucleus agree well with the ISOLTRAP value. All of them are β-endpoint data. Disagreement is found with a measurement of E. Beck et al. [33] (fig. 9 value #2). Very little information can be found in the original publication. The method used is the least-squares fit to the Fermi-Kurie plot, but it is not reported whether coincidences were used or in what way the calibration of the detector system was done. Another deviation from the ISOLTRAP datum is found in a measurement of K. Sofia et al. [30] (fig. 9 value #4). Looking more closely at the original publication, it is obvious that the assigned error is too small. The Fermi-Kurie plot was fitted using two different binnings and the final Q_β value is the weighted mean of the two. No information is given whether the background is subtracted, which might shift the endpoint. In the same publication the same method applied (here even in γ-coincidence) to an other nucleus leads to an error seven times higher (for $^{121}Xe\,\Delta E = 20\,keV$, for $^{123}Xe\,\Delta E = 140\,keV$). The value taken for AME95 is the weighted mean of those measurements. They are now excluded from the evaluation and marked as "Well-documented data which disagree with other well-documented values".

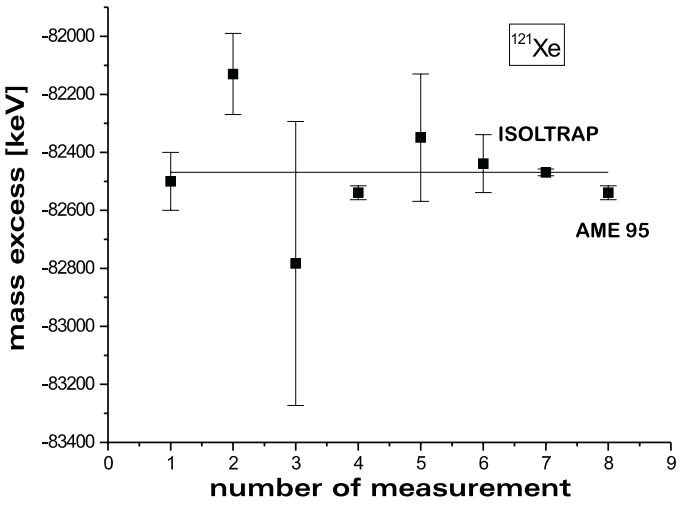

Fig. 9. Comparison of the ISOLTRAP value for ^{121}Xe with previously measured data of the mass excess. The line indicates the ISOLTRAP value. Measurement #1 [30], #2 [33], #3 [28], #4 [29], #5 [31], #6 [32].

^{120}Xe: For ^{120}Xe five mass-measurements were carried out before. One of them was exclusively (fig. 10 value #1) used for the AME95. However the error-value was modified from the original publication of F. Münnich et al. [35] where the assigned error is $200\,keV$ and the one used for AME95 is $40\,keV$. The Q_β-determination method applied here is by EC/β^+-ratio measurement. This is based on various assumptions like that energy and parity of the ground state of ^{120}I are well known and also that there is no feeding by other more abundant positrons of this state which would consequently change that rate. Further discussion with the authors of the AME [36] led to an exclusion of this value, due to some uncertainties of those assumptions. The other masses agree well within errorbars (fig. 10 value #3 and #5) or the error in the original publication seem to be too small. The latter is the case for [38] (fig. 10 value #2) where the value is derived by a linear fit to a Fermi-Kurie plot. For the other disagreeing value (#4) no documentation is available [31].

^{119}Xe: The mass of this isotope given in the atomic mass evaluation of 1995 is the weighted average of two measurements [33] and [31]. Both values and the average agree well within errors with the datum presented here.

^{118}Xe: The value of ISOLTRAP is in agreement with the measured value [34] taken for AME95. Another measurement [33] with smaller errors is excluded and marked: "Data from incomplete reports, at variance with other data or with systematics" in the documentation of the new AME, due to little information given in the publication.

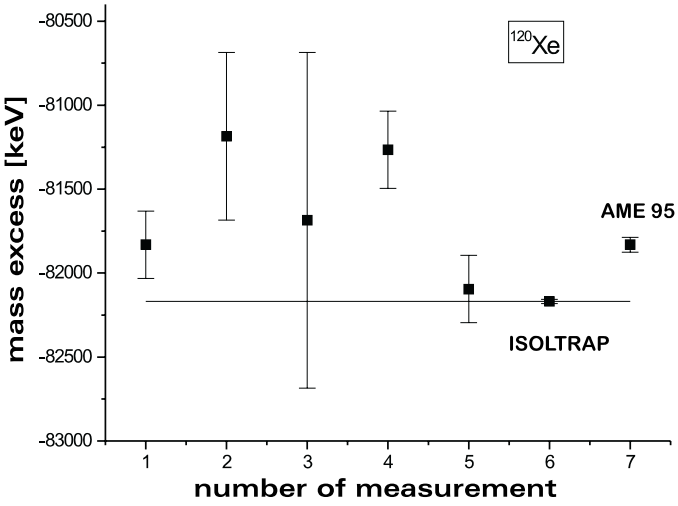

Fig. 10. Comparison of the ISOLTRAP value for ^{120}Xe with previously measured data of the mass excess. The line indicates the value reported in this work. Measurement #1 [35], #2 [32], #3 [37], #4 [38], #5 [31].

^{117}Xe: Two measurements were performed on the mass of this isotope. The ISOLTRAP datum agrees well with the previous data [40] and [41].

^{116}Xe: In the AME 95 an estimate from systematic trends is given. There existed however a measurement by Gowdy et al. [39] where the value is derived from the difference of two Fermi-Kurie plots. For the AME this value was regarded as differing too much from the systematic trend and therefore marked as "Nuclei for which masses estimated from systematic trends are thought better than the experimental masses". Agreement with this experimental datum and the value from systematics is found within the estimated uncertainty of the extrapolation.

^{115}Xe: For the isotope ^{115}Xe there were two values documented [37,42] in the AME 95, but the given mass is an estimation from systematic trends. The experimental masses were regarded as in the case of ^{116}Xe as not reliable enough. The ISOLTRAP value agrees well with these measurements and the value derived from systematic trends. By looking at the original publication of D'Auria et al. [37] it seemed that the datum used in the tables is rather the systematic prediction in their work than their measured value. For the new documentation this is changed to a mass $400\,keV$ more bound as read from the graph.

^{114}Xe: No measurements existed for this isotope. The mass reported in this work is within the expectation from systematics.

References

1. E.W. Otten in: "Treatise on heavy-ion science, Vol. 8", ed. D.A. Bromley, Plenum Publishing Coperation (1989), p.535.
2. H. Raimbault-Hartmann et al., Nucl. Inst. Meth. B **126**, 378 (1997).
3. G. Bollen et al., Nucl. Instr. Meth. A **368**, 675 (1996).
4. F. Herfurth et al., Nucl.Instr.Meth. (to be published).
5. G. Savard et al., Phys. Lett. A **158**, 247 (1991).
6. M. König et al., Int. J. Mass. Spectr. Ion. Proc. **142**, 95 (1995).
7. H. Stolzenberg et al., Phys. Rev. Lett. **65**, 3104 (1990).
8. F. Ames et al., Nucl. Phys. A **651**, 3 (1999).
9. D. Beck et al., Euro. J. Phys. sent for publication.
10. G. Audi and A.H. Wapstra, Nucl. Phys. A **595**, 409 (1995).
11. E. Kugler et al., Nucl. Instr. Meth. B **70**, 41 (1992).
12. ISOLDE User's Guide, ed. H.-J. Kluge, CERN Yellow Report 86-05, CERN, Genf (1986)
13. O.C. Johnson (privat communication)
14. T. Bjornstat et al., Phycsica Scripta **34**, 578 (1986).
15. G. Bollen et al., J. Appl. Phys. **68**, 4355 (1990).
16. L.S. Brown and G. Gabrielse, Rev. Mod. Phys. **58**, 233 (1986).
17. D. Beck et al., Nucl. Inst. Meth. B **126**, 374 (1997).
18. G. Bollen et al., Phys. Rev. C **46**, R2140 (1992).
19. M.P. Bradley et al., Phys. Rev. Lett. **83**, 4510 (1999).
20. Z. Patyk et al., Phys. Rev. A **59**, 704 (1999).
21. P. Möller et al., At. Data Nucl. Data Tables **39**, 225 (1988)
22. W. Borchers, Ph.D. thesis, University of Mainz, 1989.
23. T.R. Werner and J. Dudek, At. Data Nucl. Data Tables **54**, 1 (1995).
24. P.F. Mantinca and W.B. Walters, Phys. Rev. C **53**, R2586 (1996).
25. F. Becker et al., Eur.Phys.J. A **4**, 103 (1999).
26. R. Fossion et al., Nucl. Phys. A (2001) in press.
27. H. B. Mathur et al., Phys. Rev. A **96**, 126 (1975).
28. R.B. Moore, Bulletin of the Am. Phys. Soc. p.68, 1960.
29. L. Weestgard et al.,Z. Phys. A **275**, 127 (1975).
30. K. Sofia et al., Phys. Rev. C **24**, 1615 (1981).
31. R.F. Parry, Ph.D. thesis, University of California at Berkeley, 1983.
32. G.D. Alkazov et al., Z. Phys. A **344**, 425 (1993).
33. E. Beck et al.,in Proc. Int. Conf. on the Properties of Nuclei Far From the Region of Beta-Stability, Lysin, 1970, CERN 70-30 (1970) Vol.1, p.353.

34. J.M. D'Auria et al.,in Proc. Int. Conf. on the Properties of Nuclei Far From the Region of Beta-Stability, Cargese, 1976, CERN 76-33 (1976) Vol.1, p.100
35. F. Münnich et al., Nucl. Phys. A **224**, 437 (1974).
36. A. Wapstra (privat communication).
37. J.M. D'Auria et al., Nucl. Phys. A **301**, 397 (1978).
38. T. Batsch et al.,in Proc. Int. Conf. on the Properties of Nuclei Far From the Region of Beta-Stability, Cargese, 1976, CERN 76-33 (1976) Vol.1, p.106
39. G.M. Gowdy et al., Phys. Rev. C **13**, 1601 (1976).
40. P. Hornshoj et al., Nucl. Phys. A **187**, 599 (1972).
41. R.S. Lee et al., Phys. Rev. C **32**, 277 (1985).
42. D.D. Bogdanov et al., Phys. Lett. A **71** , 67 (1977).